Cesium Lead Bromides—Structural, Electronic and Optical Properties

Aneer Lamichhane and N. M. Ravindra

Abstract In recent years, it has been found that lowering the dimensionality of halide perovskites leads to enhanced photoluminescence and stability than their three-dimensional counterparts. Further, the change in the dimensionality of an inorganic halide perovskite can evoke surprising ramifications to its intrinsic behavior. The dimensionality in perovskites is governed by its octahedral cages. In zero-dimensional perovskites, the octahedral cages are discrete, whereas in two-dimensional perovskites, they are connected with one another resulting in the formation of a layer. Likewise, in three-dimensional perovskites, the octahedral cages share the corner atoms with each other. This study describes the two-dimensional counterpart of cesium lead bromide perovskites. The structural, electronic and optical properties, in conjunction with their three-dimensional structure, are presented. The emergence of new physical phenomena with respect to the decreasing dimensionality of cesium lead bromide perovskites is analyzed.

Keywords $CsPbBr_3$, $CsPbBr_4$, $CsPb_2Br_5$ · Structural properties · Electronic properties · Optical properties

Introduction

Perovskite solar cells have gained notoriety in the last few years as their light-harvesting capacity has been augmented from 3.8% in 2009 to over 24.2% in 2019 [1]. Despite the demonstration of increasing efficiency of perovskite solar cells in a short time, there are several issues such as fabrication processes, stability, degradation, predictability in behavior, durability, toxicity that have hindered their use in the commercial realm [2–4]. Methylammonium lead halide has been extensively studied

A. Lamichhane (✉) · N. M. Ravindra (✉)
Interdisciplinary Program in Materials Science & Engineering, New Jersey Institute of Technology, Newark, NJ 07102, USA
e-mail: al593@njit.edu

N. M. Ravindra
e-mail: nmravindra@gmail.com

TMS 2021 150th Annual Meeting & Exhibition Supplemental Proceedings,
The Minerals, Metals & Materials Series,
https://doi.org/10.1007/978-3-030-65261-6_1

from the very beginning due to its potential as a perovskite solar cell material [5, 6]. However, this material deteriorates rapidly when exposed to light, heat, air or moisture [7, 8]. As an alternative to methylammonium lead halide, it has been found that lead-based and tin-based inorganic halide perovskites show better stability under external conditions and qualify as suitable materials for solar cells and other optoelectronic devices [9–12]. From the environmental perspective, tin-based perovskites are considered as a better choice than lead-based perovskites [13]. Nevertheless, the efficiency and stability of tin-based perovskites are inferior. Furthermore, it has been found that lead-based perovskite solar cells pose a minor environmental hazard [14–17]. Among several inorganic halide perovskites, cesium lead bromide, $CsPbBr_3$, shows promise as a candidate for the fabrication of solar cells and optoelectronic devices due to its stability, inherent direct band gap, broad absorption spectrum and good transport properties [18–20].

In recent years, it has been found that lowering the dimensionality of halide perovskites leads to enhanced photoluminescence and stability than their three-dimensional counterparts [21–24]. Further, the change in the dimensionality of an inorganic halide perovskite can evoke surprising ramifications to its intrinsic behavior. The dimensionality in perovskites is governed by their octahedral cages. In zero-dimensional perovskites, the octahedral cages are discrete, whereas they are connected with one another forming a layer in two-dimensional perovskites. Likewise, in three-dimensional perovskites, the octahedral cages share the corner atoms with each other. Generally, 2D perovskites are synthesized by inserting some suitable chemical that sits in the intercalated region and acts as a spacer between the layered structures. This technique is profound in 2D organic–inorganic hybrid perovskites. Moreover, the variation of such a spacer not only produces the desired stability to the structure but also yields different functionalities of significant interest to the required 2D system. This is illustrated in Fig. 1.

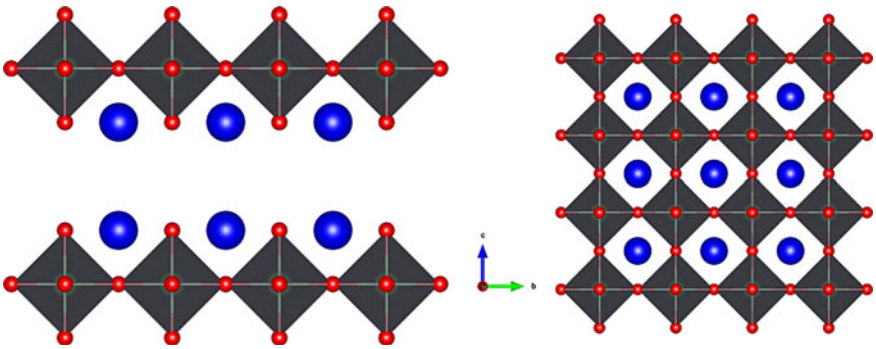

Fig. 1 Illustration showing the role of intercalated atoms as a spacer between the layer of octahedral cages in 2D (left) perovskites whereas the corner atoms link octahedral cages in all directions in 3D (right) perovskites. (Color figure online)

This paper describes the two-dimensional (2D) counterpart of $CsPbBr_3$. One plausible model for 2D-$CsPbBr_3$ would be Ruddlesden–Popper (RP) phase [25]—Cs_2PbBr_4. Unfortunately, the RP phase is not so frequent in halide perovskites in contrast to oxide perovskites [26]. Nevertheless, it is of interest to proceed with the theoretical study of RP phase of $CsPbBr_3$. On the other hand, the most likely second model for 2D counterpart of $CsPbBr_3$ would be ternary halogen-plumbate $CsPb_2Br_5$. In contrast to Cs_2PbBr_4, $CsPb_2Br_5$ can be synthesized at room temperature, different from $CsPbBr_3$ which requires a higher temperature. The first report on the synthesis of $CsPb_2Br_5$ was probably mentioned by Yu et al. [27] describing its efficient photoluminescence in the visible region (512 nm) with a quantum yield of 87%. In the paper of Sun et al. [28], the authors have reported that $CsPb_2Br_5$ results as a byproduct during the synthesis of $CsPbBr_3$, yielding higher photoluminescence by transitioning to $CsPb_2Br_5$. However, the work of Jiang et al. [29] has some contradiction by reporting $CsPb_2Br_5$ as an indirect band gap material with inactive photoluminescence. Further, Zhang et al. [30], in their paper, have clarified from the luminescence mechanism that $CsPb_2Br_5$ exhibits a band edge emission in the ultraviolet region and photoluminscence is associated with $CsPbBr_3$ byproduct in $CsPb_2Br_5$.

The need for a theoretical study of Cs-Pb-Br variants is significant due to the complexity in the synthesis and characterization of these materials. The aim of this paper is to study the structural, electronic and optical properties of 3D-$CsPbBr_3$ in conjunction with its 2D counterparts both RP phase Cs_2PbBr_4 and $CsPb_2Br_5$, utilizing the framework of density functional theory (DFT). The emergence of new physical phenomena with respect to the decreasing dimensionality of $CsPbBr_3$ is analyzed. It is anticipated that this work will be beneficial in the design and fabrication of solar cells and other potential optoelectronic devices.

Computational Details

This work utilizes first principles calculations based on DFT in which projector augmented wave (PAW) method was implemented using the Vienna Ab initio Simulation Package (VASP) [31, 32]. All the calculations were performed within the generalized gradient approximation (GGA) using Perdew, Burke and Ernzerhof (PBE) as exchange-correlation functional [33, 34]. The plane wave basis functions with large cut off energy—400 eV (greater than 1.3 times the maximum cut off energy) were used in all the three variants of Cs-Pb-Br along with a sufficiently large Monkhorst K-mesh for Brillouin zone integration. The lattice optimizations were performed with total energy convergence criteria of 10^{-6} eV and final force acting on each atom smaller than 0.02 eV/Å. The resultant optimized structures, along with the lattice parameters, are summarized in Table 1. For post processing, simulation tools such as Vesta [35], Vaspkit [36], Phonopy [37] and Sumo [38] are used in this study.

Table 1 Calculated structure of unit cell geometry with lattice parameters (a, b, c) along with their corresponding literature values in Angstrom

Material	Crystal system	Space group	Unit cell dimensions	Others work Experimental (Theoretical)
$CsPbBr_3$	Orthorhombic	Pnma (62)	$a = 8.34$, $b = 8.40$ $c = 11.97$	$a = 8.21$, $b = 8.25$ $c = 11.76$ [39]
Cs_2PbBr_4	Tetragonal	I4/mmm (139)	$a = b = 5.97$ $c = 18.33$	($a = b = 5.95$ $c = 18.19$) [40]
$CsPb_2Br_5$	Tetragonal	I4/mcm (140)	$a = b = 8.61$ $c = 15.47$	$a = b = 8.49$ $c = 15.19$ [41]

Results and Discussion

Structure and Stability

The computed structure of $CsPbBr_3$ crystallizes in the orthogonal space group of Pnma (62) and its 2D counterpart Cs_2PbBr_4 and $CsPb_2Br_5$ in the tetragonal space group of I4/mmm (139) and I4/mcm (140), respectively. Their structures are shown in Fig. 2.

$CsPbBr_3$ has interconnected or corner-sharing octahedron cage $[BX_6]^{-1}$ and Cs^{+1} residing at the center formed by eight such octahedral cages, whereas they are disjoint in Cs_2PbBr_4. Similarly, the structure of $CsPb_2Br_5$ reveals that Cs^+ resides in the intercalated region of $[Pb_2Br_5]^-$ layers. Further, the stability of these molecules can be verified by calculating their cohesive energy. The cohesive energy per atom (ΔE_c) for any molecule, say $A_aB_bX_x$, is quantified through the relation,

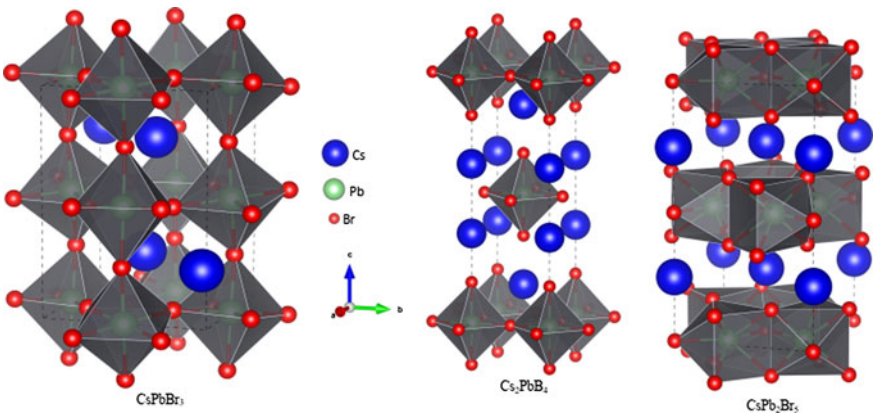

Fig. 2 Structure of 3D and 2D variants of Cs-Pb-Br. (Color figure online)

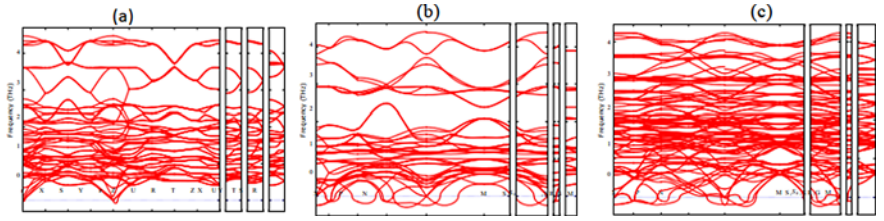

Fig. 3 Phonon dispersion diagram-**a** $CsPbBr_3$, **b** Cs_2PbBr_4 and **c** $CsPb_2Br_5$ under harmonic approximation. (Color figure online)

$$\Delta E_c(A_aB_bX_x) = \frac{aE(A) + bE(B) + xE(X) - E(A_aB_bX_x)}{a + b + x} \tag{1}$$

where $E(i)$, $i = A, B, X$ is the energy of an isolated atom i and $E(A_aB_bX_x)$ represents the total energy of $A_aB_bX_x$. The calculated values of cohesive energy per atom in eV for $CsPbBr_3$, Cs_2PbBr_4 and $CsPb_2Br_5$ are 2.89, 2.87 and 2.88, respectively. Therefore, it appears easy to dissociate Cs_2PbBr_4 among the three compounds of *Cs-Pb-Br*. Moreover, the orthorhombic phase is possibly the ground-state structures of $CsPbBr_3$, and tetragonal phases of their 2D counterparts are unstable at 0 K temperature. This can be seen by the presence of soft modes in their phonon dispersion diagram, as illustrated in Fig. 3. It has been reported that the stability can be affected by temperature as well as with the number of layers, in the case of 2D [42, 43]. Henceforth, one has enough room to suspect that these tetragonal structures might be stable at room temperature or higher, unless they have low phase transition temperature.

Electronic Properties

For simulating their electronic properties, we have computed the band structures, the total density of states (DOS) and partial density of states (PDOS); these are shown in Figs. 4(i) and (ii). One can notice that except $CsPb_2Br_5$, the other variants show direct band gap. Due to heavy atom Pb, the spin-orbit coupling (SOC) is included in all our calculations. In all three variants of *Cs-Pb-Br*, there is no significant change in the topography of the valence band with the inclusion of SOC. However, to demonstrate the conduction band degeneracy or split due to SOC, an illustration has been shown for $CsPb_2Br_5$. The calculated values of the band gap with SOC and without SOC, along with their literature values, are shown in Table 2.

It is well known that DFT calculations, using standard functional, severely underestimate the band gap, and due to the intrinsic error cancellation between SOC and neglect of quasi-particle corrections, the band gap computed without SOC has higher proximity to the correct value. Further, the orbital contribution of the valence band maximum (VBM) and the conduction band minimum (CBM) can be analyzed from

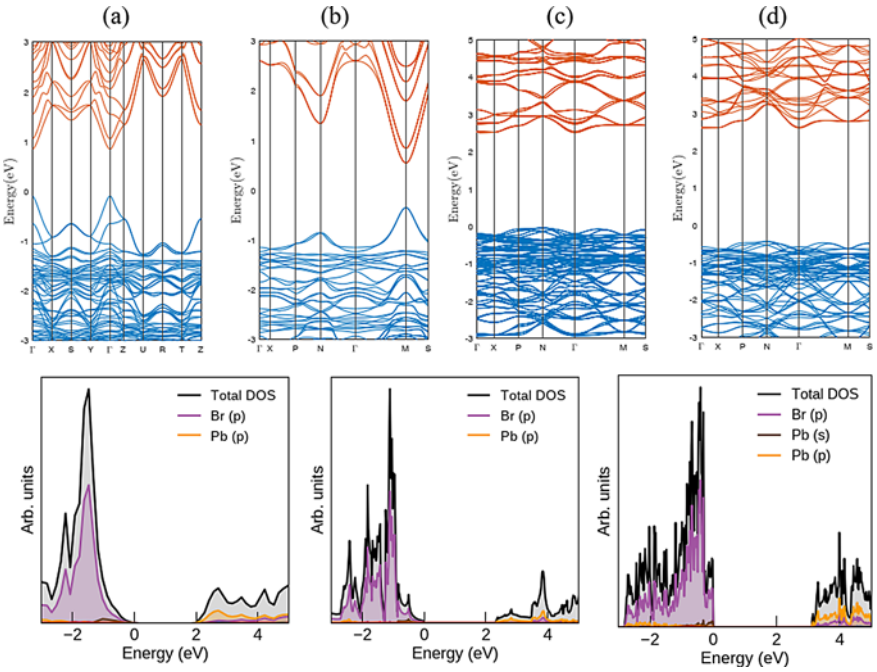

Fig. 4 (i). Top—Calculated band structure diagrams with SOC-**a** $CsPbBr_3$, **b** Cs_2PbBr_4. **c** and **d** represent $CsPb_2Br_5$ with SOC and WSOC (without SOC), respectively. (ii). Bottom—Their corresponding DOS and PDOS are shown. (Color figure online)

Table 2 Calculated values of band gap (E_g) with SOC and WSOC along with their corresponding literature values in electron volts

Material	E_g *SOC*; *WSOC*	Experimental; Theoretical
$CsPbBr_3$	0.95; 2.0	2.25 [44]; 2.16 [45]
Cs_2PbBr_4	0.98; 2.26	−; 2.29 [46]
$CsPb_2Br_5$	2.55; 3.04	3.87 [47]; 3.08 [45]

their DOS and PDOS. In all three variants, the VBM is dominated by Br p state and the CBM mainly constitute Pb p state. It is interesting to note that Cs has no direct contribution to the band edge state.

The absorption of photons in halide pervoskite solar cells leads to the generation of electrons and holes. These charge carriers are coupled with each other via Coulomb interaction to form quasiparticles in the form of excitons. The effective mass (m^*) is estimated by the parabolic fitting of energy (E) with momentum (k),

$$m^* = h^2 \left[\frac{\partial^2 E}{\partial k^2} \right]^{-1} \tag{2}$$

and the exciton binding energy (E_b) is calculated by utilizing the Wannier exciton model [48],

$$E_b = \frac{2\mu e^4}{(h8\pi\varepsilon(\infty))^2} \tag{3}$$

where μ and $\hbar$ are the reduced effective mass and Planck constant, respectively, e is the electronic charge and ε (∞) is the permittivity at high wavelength limit (low frequency—static). In the case of $CsPbBr_3$, the computed values of m_e^* and m_h^*, under the effect of SOC, are 0.157 m_e and 0.124 m_e, respectively, and E_b is 51.72 meV. The literature values of m_e^*/m_h^* are slightly greater/less than 0.2 m_e, indicating $m_h^* < m_e^*$ [49]. The calculated values of exciton binding energy for $CsPbBr_3$ are in the range of 27-63 meV [50]. Likewise, the values of m_e^*, m_h^* and E_b for Cs_2PbBr_4 are 0.17 m_e, 0.19 m_e and 102.5 meV, respectively. The values of m_e and m_h for Cs_2PbBr_4 are 0.194 m_e and 0.316 m_e, respectively [51]. Similarly, for $CsPb_2Br_5$, the values of m_e^*, m_h^* and E_b are 0.52 m_e, 2.41 m_e and 292.30 meV, respectively. It should be noted that the high value of m_h^* can be justified by the flat valence band, as shown in Fig. 4c and d. The relative permittivity values, used in the calculations for $CsPbBr_3$, Cs_2PbBr_4 and $CsPb_2Br_5$, are 4.29, 3.45 and 4.47, respectively. These values are the geometric mean of their respective anisotropic values.

Optical Properties

For investigating the optical properties, the absorption coefficient spectra have been studied for all the three variants of *Cs-Pb-Br*. The absorption spectra of materials are of paramount significance as the first and foremost criterion for solar cells should exhibit very high values of the absorption coefficient in the visible range of the solar spectra. Secondly, they play a major role in determining the thickness of cells and therefore in influencing the aspects of cell design. For instance, materials having a higher absorption coefficient are not only suitable for solar cells, but also comparatively thin cells can be designed. The absorption coefficients of materials depend on the frequency of incident photons. The absorption spectral characteristics of $CsPbBr_3$, Cs_2PbBr_4 and $CsPb_2Br_5$ are shown in Fig. 5. The absorption coefficients were calculated from frequency (ω) dependent dielectric functions, $\varepsilon(\omega) = \varepsilon_1(\omega) + i\varepsilon_2(\omega)$ according to the relation [52],

$$\alpha(\omega) = \frac{2\omega}{c}\left[\frac{(\varepsilon_1^2(\omega) + \varepsilon_2^2(\omega))^{\frac{1}{2}} - \varepsilon_1(\omega)}{2}\right]^{\frac{1}{2}}, \tag{4}$$

The absorption edge values found in the literature for $CsPbBr_3$ and $CsPb_2Br_5$ are 2.4 eV [53] and 3.26 eV [54], respectively, which indeed agree well with our

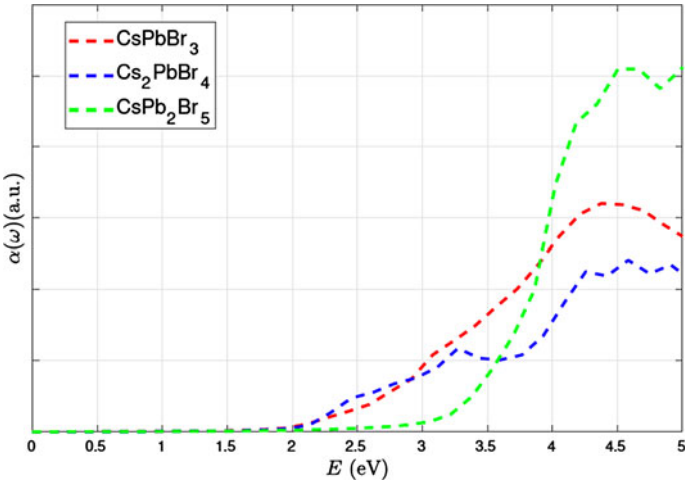

Fig. 5 Calculated absorption coefficients of *Cs-Pb-Br* variants in 100 directions. $CsPbBr_3$ is anisotropic in all directions, whereas its counterparts Cs_2PbBr_4 and $Cs_2Pb_2Br_5$ are isotropic in 100 and 010 directions. (Color figure online)

computed values. It can be seen that there is no absorption below the band edge of these materials. $CsPbBr_3$ and Cs_2PbBr_4 show broad absorption ranging from the visible to UV region, whereas $CsPb_2Br_5$ shows absorption prominent in the UV region. Therefore, $CsPbBr_3$ and Cs_2PbBr_4 are more suitable for photovoltaic applications.

Conclusions

In summary, we have studied the structural, electronic and optical properties of $CsPbBr_3$ along with its 2D variants-Cs_2PbBr_4, $CsPb_2Br_5$. There is no significant difference in the cohesive energy of these compounds. All of them show anisotropy, and their band structures show noticeable variation in the conduction band region, due to spin-orbit coupling. Except $CsPb_2Br_5$, the other two variants possess intrinsic direct band gap. The optical properties reveal that $CsPbBr_3$ and Cs_2PbBr_4 have absorption edge in the wavelength range of visible to low UV, while $CsPb_2Br_5$ shows dominant absorption in the UV region. The calculations show that the excitons are loosely bound in $CsPbBr_3$ than its 2D counterparts.

Acknowledgements The authors acknowledge with thanks the support of the Academic & Research Computing Systems, NJIT, especially Dr. Glenn (Gedaliah) Wolosh and Dr. Kevin Walsh.

References

1. Selvakumar Pitchaiya, Muthukumarasamy Eswaramoorthy, Nandhakumarand Natarajan, Agilan Santhanam, Vijayshankar Asokan, Venkatraman Madurai Ramakrishnan, Balasundaraprabhu Rangasamy, Senthilarasu Sundaram, Punniamoorthy Ravirajan, and Dhayalan Velauthapillai (2020) Perovskite solar cells: A porous graphitic carbon based hole transporter/counter electrode material extracted from an invasive plant species eichhornia crassipes. *Scientific Reports*, 10(1):6835
2. Djurišić AB, Liu FZ, Tam HW, Wong MK, Ng A, Surya C, Chen W, and He ZB (2017) Perovskite solar cells—an overview of critical issues. *Progress in Quantum Electronics*, 53:1–37
3. Meng Lei, You Jingbi, Yang Yang (2018) Addressing the stability issue of perovskite solar cells for commercial applications. *Nature Communications* 9(1):5265
4. Yaoguang Rong, Yue Hu, Anyi Mei, Hairen Tan, Makhsud I. Saidaminov, Sang Il Seok, Michael D. McGehee, Edward H. Sargent, and Hongwei Han (2018) Challenges for commercializing perovskite solar cells. *Science*, 361(6408)
5. Kojima Akihiro, Teshima Kenjiro, Shirai Yasuo, Miyasaka Tsutomu (2009) Organometal halide perovskites as visible-light sensitizers for photovoltaic cells. J Am Chem Soc 131(17):6050–6051
6. Quarti Claudio, Mosconi Edoardo, De Angelis Filippo (2014) Interplay of orientational order and electronic structure in methylammonium lead iodide: Implications for solar cell operation. Chem Mater 26(22):6557–6569
7. Jun Hong Noh, Im Sang Hyuk, Heo Jin Hyuck, Mandal Tarak N., and Seok Sang Il (2013) Chemical management for colorful, efficient, and stable inorganic–organic hybrid nanostructured solar cells. *Nano Letters*, 13(4):1764–1769
8. Tanzila Ava, Abdullah Mamun, Sylvain Marsillac, and Gon Namkoong (2019) A review: Thermal stability of methylammonium lead halide based perovskite solar cells. *Applied Sciences*, 9:188
9. Azat F. Akbulatov, Lyubov A. Frolova, Nadezhda N. Dremova, Ivan Zhidkov, Vyacheslav M. Martynenko, Sergey A. Tsarev, Sergey Yu. Luchkin, Ernst Z. Kurmaev, Keith J. Aldoshin, Sergey M.and Stevenson, and Pavel A. Troshin (2020) Light or heat: What is killing lead halide perovskites under solar cell operation conditions? *The Journal of Physical Chemistry Letters*, 11(1):333–339
10. Zou Shibing, Li Feng (2020) Efficient all-inorganic CsPbBr 3 perovskite solar cells by using CdS/CdSe/CdS quantum dots as intermediate layers. *Journal of Nanomaterials* 2020:7946853
11. Konstantakou Maria, Stergiopoulos Thomas (2017) A critical review on tin halide perovskite solar cells. J. Mater. Chem. A 5:11518–11549
12. Pablo Boix, Shweta Agarwala, Teck Ming Koh, Nripan Mathews, and Subodh Mhaisalkar (2015) Perovskite solar cells: Beyond methylammonium lead iodide. *The Journal of Physical Chemistry Letters*, 6:898–907(150213091342008)
13. Shi Zejiao, Guo Jia, Chen Yonghua, Li Qi, Pan Yufeng, Zhang Haijuan, Xia Yingdong, Huang Wei (2017) Lead-free organic–inorganic hybrid perovskites for photovoltaic applications: Recent advances and perspectives. Adv Mater 29(16):1605005
14. Luc´ıa Serrano-Luja´n, Nieves Espinosa, Thue Trofod, Jose Abad, Antonio Urbina, and Frederik Krebs (2015) Tin- and lead-based perovskite solar cells under scrutiny: An environmental perspective. *Advanced Energy Materials*
15. Gao Fengqiang, Li Chunhai, Qin Liang, Zhu Lijie, Huang Xin, Liu Huan, Liang Liming, Hou Yanbing, Lou Zhidong, Yufeng Hu, Teng Feng (2018) Enhanced performance of tin halide perovskite solar cell by addition of lead thiocyanate. RSC Adv. 8:14025–14030
16. Billen Pieter, Leccisi Enrica, Dastidar Subham, Li Siming, Lobaton Liliana, Spatari Sabrina, Fafarman Aaron T, Fthenakis Vasilis M, Baxter Jason B (2019) Comparative evaluation of lead emissions and toxicity potential in the life cycle of lead halide perovskite photovoltaics. *Energy* 166:1089–1096

17. Syed Azkar Ul Hasan, David S. Lee, Sang Hyuk Im, and Ki-Ha Hong (2020) Present status and research prospects of tin-based perovskite solar cells. *Solar RRL*, 4(2):1900310
18. Xin Li, Yao Tan, Hui Lai, Shuiping Li, Ying Chen, Suwei Li, Peng Xu, and Junyou Yang (2019) All-inorganic CsPbBr3 perovskite solar cells with 10.45% efficiency by evaporation-assisted deposition and setting intermediate energy levels. *ACS Applied Materials & Interfaces*, 11(33):29746–29752
19. Juan Li, Rongrong Gao, Fei Gao, Jie Lei, Haoxu Wang, Xin Wu, Jianbo Li, Hao Liu, Xiaodong Hua, and Shengzhong (Frank) Liu (2020) Fabrication of efficient $CsPbBr_3$ perovskite solar cells by single-source thermal evaporation. *Journal of Alloys and Compounds*, 818:152903
20. Zeng Junpeng, Zhou Hai, Liu Ronghuan, Wang Hao (2019) Combination of solution-phase process and halide exchange for all-inorganic, highly stable $CsPbBr_3$ perovskite nanowire photodetector. *Science China Materials* 62(1):65–73
21. Niu Tingting, Ren Hui, Bo Wu, Xia Yingdong, Xie Xiaoji, Yang Yingguo, Gao Xingyu, Chen Yonghua, Huang Wei (2019) Reduced-dimensional perovskite enabled by organic diamine for efficient photovoltaics. *The Journal of Physical Chemistry Letters* 10(10):2349–2356
22. Yulia Lekina and Ze Xiang Shen (2019) Excitonic states and structural stability in two-dimensional hybrid organic-inorganic perovskites. *Journal of Science: Advanced Materials and Devices* 4(2):189–200
23. Daniela Marongiu, Michele Saba, Francesco Quochi, Andrea Mura, and Giovanni Bongiovanni (2019) The role of excitons in 3d and 2d lead halide perovskites. *J. Mater. Chem. C*, 7:12006– 12018
24. Wancai Li, Jiaqi Ma, Xue Cheng, and Dehui Li (2020) Giant enhancement of photoluminescence quantum yield in 2d perovskite thin microplates by graphene encapsulation. *Nano Research*, Jul 2020
25. Ruddlesden SN, Popper P (1957) New compounds of the K_2NiF_4 type. *Acta Crystallogr A* 10(8):538–539
26. Yi Yu, Zhang Dandan, Yang Peidong (2017) Ruddlesden–popper phase in two-dimensional in- organic halide perovskites: A plausible model and the supporting observations. Nano Lett 17(9):5489–5494
27. Wang Kun-Hua, Liang Wu, Li Lei, Yao Hong-Bin, Qian Hai-Sheng, Shu-Hong Yu (2016) Large- scale synthesis of highly luminescent perovskite-related $CsPb_2Br_5$ nanoplatelets and their fast anion exchange. Angew Chem Int Ed 55(29):8328–8332
28. Xiaoli Zhang, Bing Xu, Jinbao Zhang, Yuan Gao, Yuanjin Zheng, Kai Wang, and Xiao Wei Sun (2016) All-inorganic perovskite nanocrystals for high-efficiency light emitting diodes: Dual-phase $CsPbBr_3$-$CsPb_2Br_5$ composites. *Advanced Functional Materials*, 26(25):4595–4600
29. Li Guopeng, Wang Hui, Zhu Zhifeng, Chang Yajing, Zhang Ting, Song Zihang, Jiang Yang (2016) Shape and phase evolution from $CsPbBr_3$ perovskite nanocubes to tetragonal $CsPb_2Br_5$ nanosheets with an indirect bandgap. Chem Commun 52:11296–11299
30. Li Jing, Zhang Huijie, Wang Song, Long Debing, Li Mingkai, Guo Yizhong, Zhong Zhicheng, Kaifeng Wu, Wang Duofa, Zhang Tianjin (2017) Synthesis of all-inorganic $CsPb_2Br_5$ perovskite and determination of its luminescence mechanism. RSC Adv. 7:54002–54007
31. Kresse G, Hafner J (1993) Ab initio molecular dynamics for liquid metals. Phys. Rev. B 47:558–561
32. G. Kresse and J. Furthmüller (1996) Efficient iterative schemes for ab initio total-energy calculations using a plane-wave basis set. Phys. Rev. B, 54:11169–11186
33. Perdew John P, Burke Kieron, Ernzerhof Matthias (1996) Generalized gradient approximation made simple. Phys Rev Lett 77:3865–3868
34. Perdew John P, Burke Kieron, Wang Yue (1996) Generalized gradient approximation for the exchange-correlation hole of a many-electron system. Phys. Rev. B 54:16533–16539
35. Momma Koichi, Izumi Fujio (2011) VESTA3 for three-dimensional visualization of crystal, volumetric and morphology data. J Appl Crystallogr 44(6):1272–1276
36. Wang Vei, Nan Xu (2019) Jin Cheng Liu, Gang Tang, and Wen-Tong Geng. A user-friendly interface facilitating high-throughput computing and analysis using VASP code, Vaspkit

37. Togo A, Tanaka I (2015) First principles phonon calculations in materials science. Scr. Mater. 108:1–5
38. Alex Ganose, Adam Jackson, and David Scanlon (2018) sumo: Command-line tools for plotting and analysis of periodic ab initio calculations. *Journal of Open Source Software*, 3:717
39. Rodová M, Brožek J, Knížek K, and Nitsch K (2003) Phase transitions in ternary caesium lead bromide. *Journal of Thermal Analysis and Calorimetry*, 71(2):667–673
40. Li Jiangwei, Qin Yu, He Yihui, Stoumpos Constantinos C, Niu Guangda, Trimarchi Giancarlo G, Guo Hang, Dong Guifang, Wang Dong, Wang Liduo, Kanatzidis Mercouri G (2018) $Cs_2PbI_2Cl_2$, all-inorganic two-dimensional ruddlesden–popper mixed halide perovskite with optoelectronic response. J Am Chem Soc 140(35):11085–11090
41. Dursun Ibrahim, DeBastiani Michele, Turedi Bekir, Alamer Badriah, Shkurenko Aleksander, Yin Jun, El-Zohry Ahmed M, Gereige Issam, AlSaggaf Ahmed, Mohammed Omar F, Eddaoudi Mohamed, Bakr Osman M (2017) $CsPb_2Br_5$ single crystals: Synthesis and characterization. Chemsuschem 10(19):3746–3749
42. Qi Meng, Yichuan Chen, Yue Yue Xiao, Junjie Sun, Xiaobo Zhang, Chang Bao Han, Hongli Gao, Yongzhe Zhang, and Hui Yan (2020) Effect of temperature on the performance of perovskite solar cells. *Journal of Materials Science: Materials in Electronics*, Feb 2020
43. Chan Myae Myae Soe, G. P. Nagabhushana, Radha Shivaramaiah, Hsinhan Tsai, Wanyi Nie, Jean-Christophe Blancon, Ferdinand Melkonyan, Duyen H. Cao, Boubacar Traore´, Laurent Pedesseau, Mikae¨l Kepenekian, Claudine Katan, Jacky Even, Tobin J. Marks, Alexandra Navrotsky, Aditya D. Mohite, Constantinos C. Stoumpos, and Mercouri G. Kanatzidis (2019) Structural and thermodynamic limits of layer thickness in 2d halide perovskites. *Proceedings of the National Academy of Sciences*, 116(1):58–66
44. Constantinos C. Stoumpos, Christos D. Malliakas, John A. Peters, Zhifu Liu, Maria Sebastian, Jino Im, Thomas C. Chasapis, Arief C. Wibowo, Duck Young Chung, Arthur J. Freeman, Bruce W. Wessels, and Mercouri G. Kanatzidis (2013) Crystal growth of the perovskite semiconductor $CsPbBr_3$: A new material for high-energy radiation detection. *Crystal Growth & Design*, 13(7):2722–2727
45. Huang ZhiPeng, Ma Bo, Wang Hao, Li Na, Liu Rui-Tong, Zhang Ze-Qi, Zhang Xiao-Dong, Zhao Ji-Hua, Zheng Pei-Zhu, Wang Qiang, Zhang Hao-Li (2020) In situ growth of 3d/2d (CsPbBr 3/CsPb2Br5) perovskite heterojunctions toward optoelectronic devices. *The Journal of Physical Chemistry Letters* 11(15):6007–6015
46. Yang Ji-Hui, Yuan Qinghong, Yakobson Boris I (2016) Chemical trends of electronic properties of two-dimensional halide perovskites and their potential applications for electronics and optoelectronics. *The Journal of Physical Chemistry C* 120(43):24682–24687
47. Zhang Zhaojun, Zhu Yanming, Wang Weiliang, Zheng Wei, Lin Richeng, Huang Feng (2018) Growth, characterization and optoelectronic applications of pure-phase large-area CsPb2Br 5 flake single crystals. J. Mater. Chem. C 6:446–451
48. Stefano Sanguinetti, Mario Guzzi, and Massimo Gurioli. 6—accessing structural and electronic properties of semiconductor nanostructures via photoluminescence. In Carlo Lamberti, editor, *Characterization of Semiconductor Heterostructures and Nanostructures*, pages 175 – 208. Elsevier, Amsterdam, 2008
49. Negar Ashari-Astani, Simone Meloni, Amir Hesam Salavati, Giulia Palermo, Michael Grätzel, and Ursula Rothlisberger (2017) Computational characterization of the dependence of halide perovskite effective masses on chemical composition and structure. *The Journal of Physical Chemistry C*, 121(43):23886–23895
50. Hamid M. Ghaithan, Zeyad A. Alahmed, Saif M. H. Qaid, Mahmoud Hezam, and Abdullah S. Aldwayyan (2020) Density functional study of cubic, tetragonal, and orthorhombic $CsPbBr_3$ perovskite. *ACS Omega*, 5(13):7468–7480
51. Yang Ji-Hui, Yuan Qinghong, Yakobson Boris I (2016) Chemical trends of electronic properties of two-dimensional halide perovskites and their potential applications for electronics and optoelectronics. The Journal of Physical Chemistry C 120(43):24682–24687
52. Yong Hua Duan and Yong Sun (2013) First-principles calculations of optical properties of Mg_2Pb. *Science China Physics, Mechanics and Astronomy*, 57:233–238

53. Hamid M. Ghaithan, Zeyad A. Alahmed, Saif M. H. Qaid, Mahmoud Hezam, and Abdullah S. Aldwayyan (2020) Density functional study of cubic, tetragonal, and orthorhombic $CsPbBr_3$ perovskite. *ACS Omega*, 5(13):7468–7480
54. Jin Mingge, Li Zhibing, Huang Feng, Wang Weiliang (2019) Electronic and optical properties of $CsPb_2Br_5$: A first-principles study. Mod Phys Lett B 33(22):1950266